Laser-Induced Decomposition and Ablation Dynamics Studied by Nanosecond Interferometry. 1. A Triazenopolymer Film

H. Furutani,[†] H. Fukumura,*[,†] H. Masuhara,*[,†] T. Lippert,[‡,§] and A. Yabe[‡]

Department of Applied Physics, Osaka University, Suita, Osaka 565, Japan, and Laser Induced Reaction Laboratory, National Institute of Materials and Chemical Research, Higashi 1-1, Tsukuba, Ibaraki 305, Japan

Received: March 27, 1997; In Final Form: June 10, 1997[⊗]

The dynamic behavior of a photoetching process of a photosensitive triazenopolymer film during and after XeF excimer laser irradiation was studied by nanosecond interferometry, accompanied with time-resolved transmission and reflectance measurements. A new optical setup for nanosecond interferometry, which was free from the disturbance of ejected products, was developed and applied. At a fluence of 250 mJ/cm^2 a slight swelling of the film and darkening of the irradiated surface was initially observed, and then the etching process of the film was brought out around the peak time of the excitation laser pulse. The etching developed during the excitation laser pulse and stopped almost at the end of the excimer laser pulse. On the other hand, at a fluence of 60 mJ/cm^2, the etching started from nearly the end of the excimer laser pulse and persisted for 50 ns. The fluence dependent etching behavior was interpreted in terms of coupled photochemical and thermal decomposition processes of the triazenopolymer.

Introduction

Laser ablation of organic solid films is a unique physicochemical phenomenon that has received much attention in the fields of photochemistry and molecular materials.[1−3] Intense pulse laser irradiation results in high-density excitation of organic chromophores, leading to morphological changes of the films.[4,5] The coupling between molecular processes and morphological changes is one of the most unique and important characteristics of laser ablation. However, both have been studied rather separately and discussed independently. Excitation energy relaxation dynamics and primary chemical processes of organic molecules in laser ablation have been investigated by using various time-resolved spectroscopies, such as fluorescence,[5,7−9] absorption,[5,8,9] Raman,[10] and IR[11] spectroscopies. Under the ablation condition, normal photophysical and photochemical processes are modified and new relaxation channels are opened. For example, it has been revealed that cyclic multiphoton absorption and mutual interactions between excited states were brought about, causing rapid temperature elevation of the polymer matrix[6,8,12] and thermal decomposition of the polymer.[6,10] On the other hand, morphological dynamics has been studied mainly with respect to ejection behavior of fragments or plume.[5,13−17] Of course the ejection dynamics is a reflection of molecular process, but its direct information is not clearly contained in the ejection behavior, since the primary molecular processes are already completed when fragments or plume ejection is brought about. Therefore, it is most desirable to correlate the molecular process with morphological changes *during* or *just after* the excitation laser pulse, from which new aspects of laser ablation mechanism will be clarified.

In order to reveal the dynamic behavior of morphological changes in the nanosecond time region, we have already developed nanosecond interferometry, which makes it possible to measure the 20−30 nm expansion and contraction of irradiated films with a time resolution of 10 ns.[18,19] Such nanosecond morphological changes of biphenyl- or pyrene-doped poly(methyl methacrylate) (PMMA) and poly(methyl acrylate) (PMA) films were successfully measured above and below the ablation threshold.[20] It was demonstrated that even below the ablation threshold, transient expansion of the polymer films emerged during the excitation pulse, which was confirmed to be thermal expansion due to the nanosecond photothermal heating by doped aromatic molecules.[18,19] The expansion dynamics was well interpreted to be consistent with the glass−rubber transition of the polymer films.[19] It was directly shown that, above the ablation threshold, expansion already started during the excitation pulse and then ejection of ablated polymer was followed explosively.[18] On the basis of these results, we have discussed the dynamic evolution from the thermal expansion to the ablation.

SCHEME 1. Chemical Structure of the Triazenopolymer

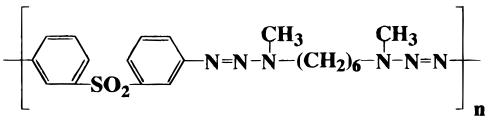

In contrast to the photothermal ablation of the doped polymer films, triazenopolymer (Scheme 1), which contains photosensitive triazenochromophore in the main chain, is reported to show a different ablation behavior.[21] It was exhibited by using a scanning electron microscope and a nanosecond imaging method that well-defined etch patterns, with no debris contaminating the polymer surface, were observed[21] and only gaseous products were explosively ejected from the irradiated film.[17] Their etching phenomena did not suggest the thermal decomposition, and direct breaking of the main chain by the excimer laser irradiation probably led to photochemical ablation.[21,22] Therefore, the triazenopolymer film is expected to show novel morphological dynamics different from doped PMMA and PMA films, which would give us clear distinction between photothermal and photochemical ablation dynamics.

In this report, decomposition dynamics of the photosensitive triazenopolymer film upon intense XeF excimer laser irradiation is studied by applying the nanosecond interferometric technique with a newly improved optical setup. On the basis of revealed

[†] Osaka University.
[‡] National Institute of Materials and Chemical Research.
[§] Present address: Los Alamos National Laboratory, CST 6, MS-J 665, Los Alamos, NM 87545.
[⊗] Abstract published in *Advance ACS Abstracts,* July 15, 1997.

S1089-5639(97)01081-5 CCC: $14.00

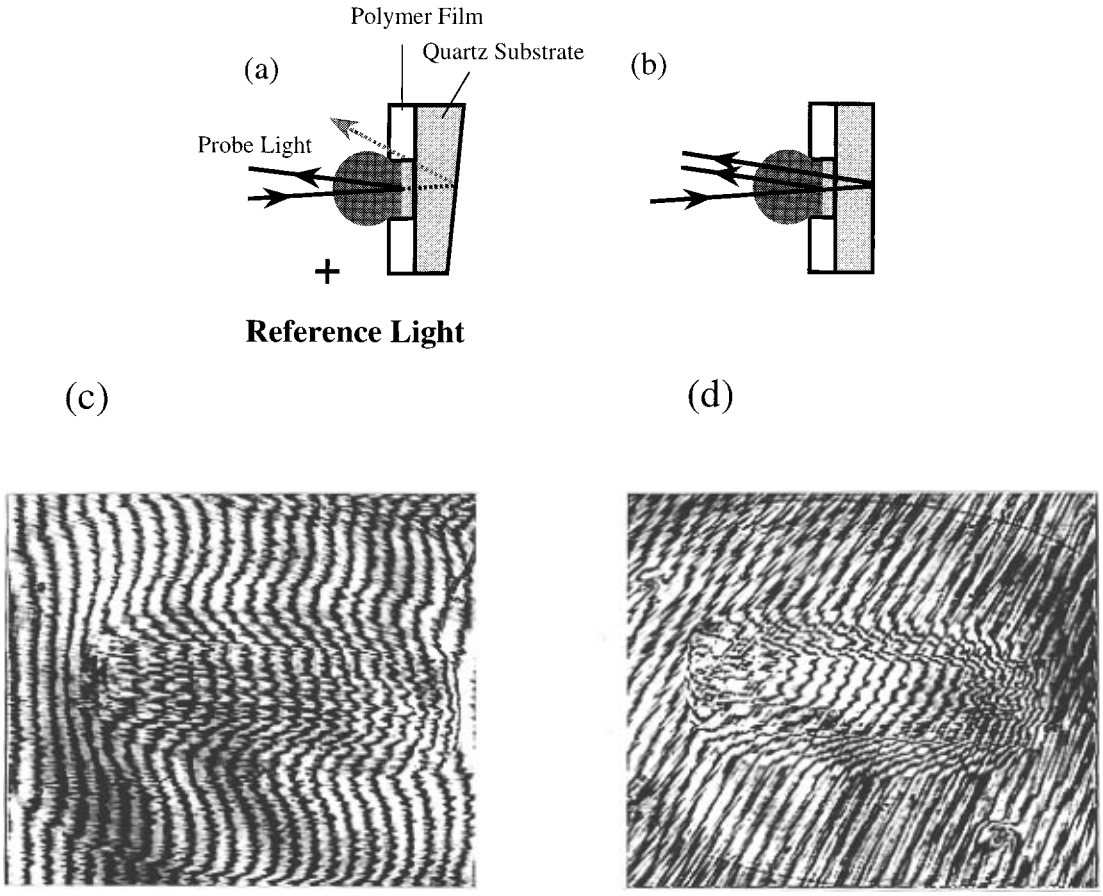

Figure 1. Optical setups of (a) the surface configuration and (b) the internal configuration. Typical interference images of the triazenopolymer film obtained with the surface configuration (c) and the internal configuration (d). Both images were acquired under the same condition at 4 μs after excitation with a fluence of 250 mJ/cm^2, and fringe movement to the right represents an etching for both configurations.

morphological dynamics as well as the obtained time-resolved transmission and reflectance, ablation mechanism and the dynamics of the triazenopolymer film are discussed in detail.

Experimental Section

Nanosecond Interferometry. The nanosecond interferometry applied here is almost the same to that of previous works,[18,19] except for the newly improved optical configuration. Briefly, a XeF excimer laser (Lambda Physik Lextra 200, 351 nm, 30 ns fwhm) was used for exciting triazenopolymer film, and a Q-switched Nd^{3+}:YAG laser (Continuum Surelite I, 532 nm, 10 ns fwhm) was a probe light source of the Michelson-type interferometer. Interference patterns were acquired by a CCD camera. The time delay (Δt) between excitation and probe laser pulses was monitored shot by shot by a digital oscilloscope (Hewlett Packard 54522A, 500 Hz). Here we define $\Delta t = 0$ when peaks of both laser pulses coincide with each other. All the data were obtained by one-shot measurement to avoid effects by exciting photoproducts formed by previous irradiation.

The optical configurations are illustrated in Figure 1a,b, which we call here *surface* and *internal* configurations, respectively. The surface configuration is the same as that in the previous works,[18,19] while the internal one is newly applied here. In the case of the surface configuration, the interference pattern results from an interference between the reference light and the light reflected at the polymer surface. In order to avoid a disturbing interference due to a light reflected at the back surface of the plate, a quartz plate whose two surfaces are not parallel was used. The interference pattern represents a surface profile of expansion or etching of irradiated polymer film properly, as far as optical properties in the pathway of probe lights are not changed appreciably. However, fragments or gaseous products are sometimes ejected from the surface of the sample film upon laser ablation, which may vary the effective optical path length of the reflected light. The disturbance by the ejected products will lead to overestimation of the surface displacement of the irradiated polymer film, since the ejected products have a higher refractive index compared to air. To overcome this problem, we have developed the *internal* configuration.

In the case of the *internal* configuration, a quartz plate whose two surfaces are quite slightly tilted are used while the reference mirror is masked. Thereby, two beams reflected at the polymer surface and at the back surface of the quartz substrate interfere with each other. As both reflected lights pass in the ejected ablation products similarly, the optical disturbance due to the ablated products can be eliminated. As the quartz substrate is not excited here by the laser irradiation, only the change of thickness or/and refractive index of the polymer film may be included in the shift of the interference patterns.

In order to demonstrate superior performance of the internal configuration, interference patterns at $+4.0$ μs after the irradiation for the same fluence of 250 mJ/cm^2, obtained by the both optical configurations, are shown in Figure 1c,d. Here fringe movement to the right represents an etching for both configurations. In the case of the internal configuration (Figure 1d), the fringe shift was observed only in the border of the irradiated area, while additional fringe deformation inside and around the irradiated area was clearly observed with the *surface* configuration (Figure 1c). This is considered to be due to inhomogeneous distribution of ejected gas molecules. The central fringe shift and the surrounding fringe deformation in Figure 1d are due to etching of the film and expanding shock wave,

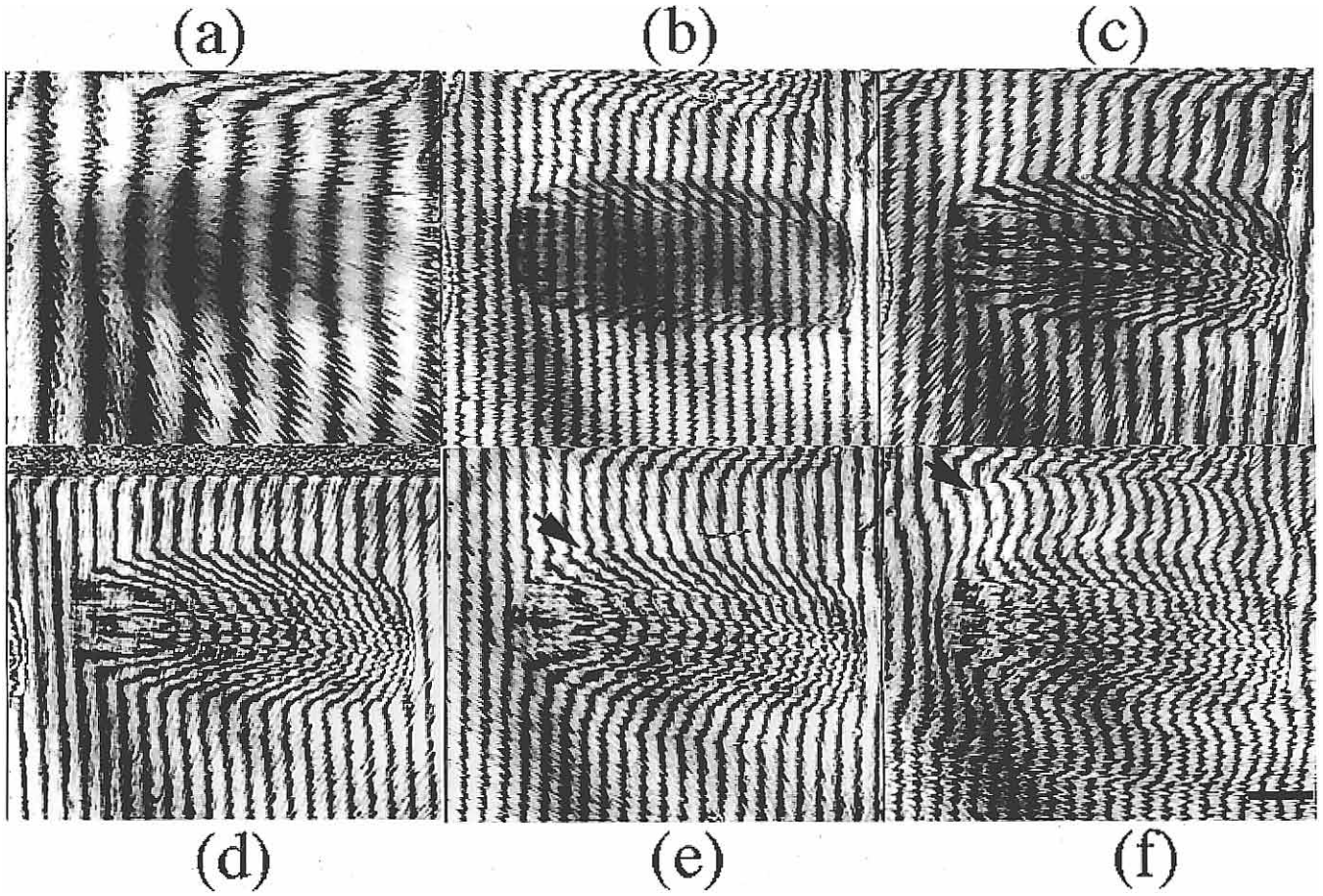

Figure 2. A series of nanosecond time-resolved interferometric images of the triazenopolymer film at a fluence of 250 mJ/cm^2, which were obtained with the surface configuration. In this case, fringe shift to the right represents an etching. Delay time (Δt): (a) -9 ns, (b) $+10$ ns, (c) $+57$ ns, (d) $+260$ ns, (e) $+1$ μs, and (f) $+3$ μs. The black bar in (f) indicates 1 mm in the image. Arrows in (e) and (f) point to the propagation front of shock wave.

respectively. Thus these two interference images clearly demonstrate that the internal configuration is useful when ablation products are ejected.

Effective Change of Optical Path Length in Sample Film. What we can extract from the fringe shift in interference patterns is a change in optical path length induced by excimer laser irradiation. As the optical path length is a product of refractive index and the real distance in the path of a probe light, in the case of the internal configuration, not only thickness change but also refractive index change of the polymer film cause variation of the optical path length. The refractive index change is considered to be induced by temperature elevation and formation of photochemical reaction products. Initially the change should occur only at the thin surface layer of the film ($\sim$90 nm) since the sample film has a high absorbance of about 4.6 in 1 μm thickness at the excitation wavelength. Because of the small change of refractive index at the thin layer, we consider that the contribution of the refractive index change is not so large and assume that the index change of the film is negligible in the calculation of thickness change even during excimer laser irradiation.

Time-Resolved Transmission and Reflectance Measurements. Visible light produced from a Xe lamp of the wavelength longer than 580 nm, selected by using a glass filter so as to not excite the triazenopolymer, was used as a probe light. Broad wavelength distribution of the probe light eliminates the transmission and reflectance changes by the interference of the probe light in the thin film. Both transmitted and reflected probe lights were detected with fast photodiodes (Hamamatu Photonics, S1722-02) and monitored with a storage oscilloscope (Hewlett Packard, 54522A).

Sample. The photosensitive triazenopolymer was synthesized by a previously reported method.[21,22] The films were prepared onto two kinds of quartz plates described above by spin coating from a tetrahydrofuran solution of the polymer. The films with a thickness of *ca.* 1 μm were baked to remove the residual solvent for more than 24 h at 50 °C under vacuum. Surface profile was measured by a depth profiler (Sloan, Dektak^2).

Results and Discussion

Time-Resolved Interference Images. In Figure 2 the interference patterns at a fluence of 250 mJ/cm^2 with the surface configuration are shown as a function of the delay time. It should be noted that all the interference fringe patterns are not similar to each other, since the interference image was acquired for a fresh surface and optical condition changed from shot to shot. In this experiment a movement of the fringe to the right side represents an etching of the polymer film, which was attained by adjusting the optical condition. Slight fringe shift to the left side, expressing a small swelling of the film, and darkening in the irradiated area were observed even at the onset of the excimer laser pulse ($\Delta t = -9$ ns). Then increasing fringe movement to the right side, expressing an etching of the polymer film, was brought about at $\Delta t = +10$ ns. The shift was increased with time. After a few tens of nanoseconds, patterns in the irradiated area are not homogeneous, which is ascribed to effects of ejected products inevitably involved in the *surface* configuration. From $\Delta t = +1.0$ μs distortion of the fringe

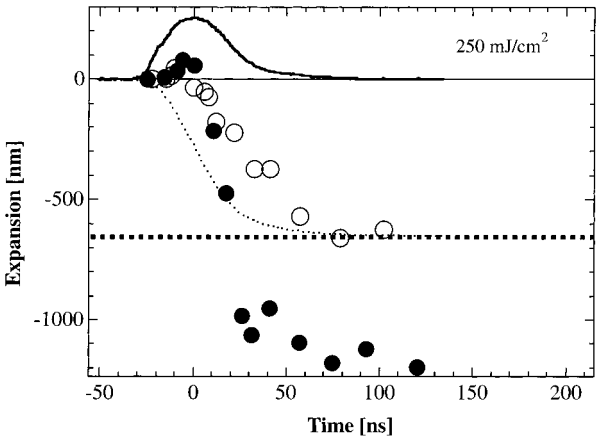

Figure 3. Etching evolution of the triazenopolymer film at the fluence of 250 mJ/cm^2 with the surface configuration (●) and with the internal configuration (○). The thick dashed line represents the permanent etched depth (∼660 nm). The thick solid curve is a profile of the excimer laser pulse, and the dotted curve is an inverse of its integration. The latter is normalized to the permanent etched depth.

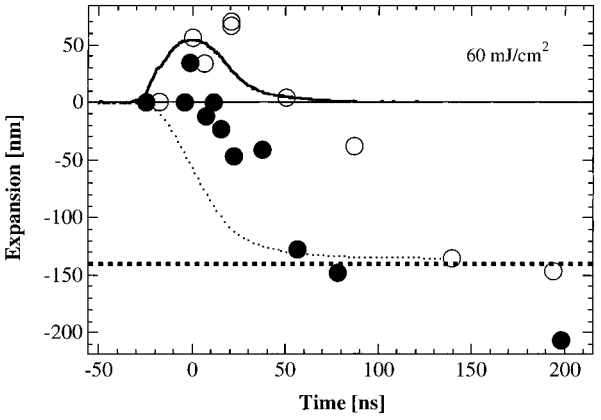

Figure 4. Etching evolution of the triazenopolymer film at the fluence of 60 mJ/cm^2 with the surface configuration (●) and with the internal configuration (○). The thick dashed line represents the permanent etched depth (∼140 nm). The thick solid curve is a profile of the excimer laser pulse, and the dotted curve is an inverse of its integration. The latter is normalized to the permanent etched depth.

pattern outside the irradiated area began to emerge and expand (arrows in the figure), which is considered to correspond to shock waves. Its propagation velocity is ∼1000 m/s, which is consistent with that observed by nanosecond photography of the present film.[17]

It is worth noting that interference patterns in the irradiated area were always visible at all delay times. This is a new case, since laser ablation of PMMA films doped with biphenyl or pyrene results in dense ejection of fragmented debris leading to shielding of probe light.[18] The present results suggest that only gaseous products are generated and ejected by the excimer laser irradiation, which is also consistent with the fact that no debris and no contaminant were observed around the etched pit.[20]

As a shift of one fringe spacing to the right corresponds to an etching of 266 nm, a half wavelength of the probe laser, expansion and etching behavior can be obtained by analyzing interference patterns at each delay time. The results obtained with two different optical setups are summarized and shown for the fluence of 250 and 60 mJ/cm^2 in Figures 3 and 4, respectively. The apparent etching obtained by the surface configuration is always deeper than that by the internal configuration. The permanent etch depth at 250 and 60 mJ/cm^2 is 600 and 140 nm, respectively. These values are in agreement with the etch depth estimated by a depth profiler.

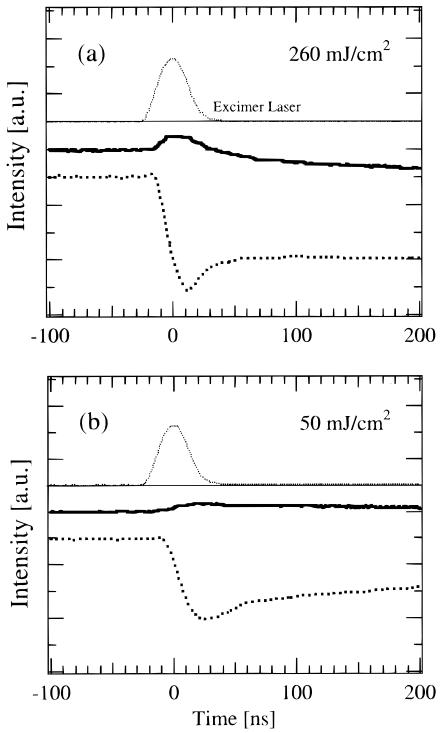

Figure 5. Time-resolved transmission and reflectance of the triazenopolymer film at (a) 250 mJ/cm^2 and (b) 50 mJ/cm^2. The thick solid and dashed curves represent transmission and reflectance changes, respectively, while the dotted one is the time profile of the excimer laser pulse.

Darkening and Small Expansion at the Early Part of the Excimer Laser Pulse. Prior to the etching, darkening and slight expansion of the film were observed from ∼ −10 ns for both 60 and 250 mJ/cm^2 as shown in Figure 2a. Such darkening upon laser ablation was reported for PMMA and poly(ethylene terephthalate) (PET) by other researchers and considered to be due to some scattering by ejected materials or a bubble formed at the irradiated surface upon laser ablation.[13,14] In this time region, the expansion dynamics measured with both *internal* and *surface* configurations were almost similar to each other as shown in Figures 3 and 4, which means that the disturbance by the ejected products is negligible. It is not considered that the triazenopolymer film was etched and decomposed products were appreciably ejected from the beginning of the excimer laser pulse, although irradiation of the excimer laser should induce decomposition of the triazenopolymer. Formation of the small bubble at the irradiated surface, leading to light scattering, also seems to be unlikely, since the fringe pattern during the darkening was not distorted but defined clearly. Therefore, we consider that mechanisms for the darkening proposed in the literature do not hold here.

For small swelling of a few tens of nanometers around 0 ns, two explanations can be given. One is a simple expansion of the triazenopolymer film, while the other is to assume that photodecomposed products such as monomers and oligomers start to expand. The latter may be more probable, although further experiments are needed to be conclusive.

In order to know the temporal evolution of the darkening, we measured time-resolved transmission and reflectance of the irradiated triazenopolymer film above 580 nm. In Figure 5(a) time-resolved transmission and reflectance are shown for a fluence of 250 mJ/cm^2. From the onset of the excimer laser pulse, reflectance began to decrease and recovered to some

extent, whereas the transmission slightly increased at first and then decreased gradually. If the darkening was caused by the light deflection or scattering by ejected gas or formed bubbles upon excimer laser irradiation, both transmission and reflectance should be attenuated. The increase of the transmission indicates that the sudden drop of the reflectance is not due to the light deflection or scattering but due to the decrease of reflectivity of the film. It is reasonable to assume that a change of the reflectivity was induced by the decrease of refractive index at the irradiated polymer surface, and photodecomposition of the triazenopolymer may cause the decrease of the refractive index. As the triazenopolymer is highly photosensitive and decomposable, triazeno chromophores in the main chain decompose rapidly losing triazeno structure upon excimer laser irradiation. As a result, the absorption spectrum of the triazeno chromophore in the ultraviolet region should be lost, and the spectral change would cause the decrease of the refractive index in the visible region not significantly but a little. As the triazenopolymer has a high absorption coefficient at the excitation wavelength, the refractive index change is estimated to take place at the surface layer of about 90 nm as mentioned above. Therefore, it is considered that the photodecomposition of triazenopolymer at the thin surface layer causes the decrease of the refractive index leading to the decrease of the reflectivity, although the photodecomposition in this time region did not bring about an appreciable change in the optical path length of the film. A slight permanent increase in transmission and a decrease followed by a small recovering were observed at 60 mJ/cm^2 as in Figure 5b.

Etching Dynamics during and after the Excimer Laser Irradiation. Etching of the film was initiated around the peak time of the excitation laser pulse; however, different time evolutions of etch depth were observed with two different configurations. The difference increased after the slight expansion. The time-resolved etch depth estimated with the surface configuration became deeper than that with the *internal* configuration and exceeded the permanent depth (the thick dashed line in the figure), while it came back to the same permanent depth after a few microseconds. As we described the characteristics of surface and internal configurations in the Experimental Section, the behavior can be well interpreted as being due to a disturbance by the products ejected from the film surface in the measurement with surface configuration. The apparent depth emerging from $\Delta t \sim +10$ ns means that explosive ejection of the decomposed polymer from the film surface started from this delay time. Qualitatively the behaviors at 250 and 60 mJ/cm^2 were similar to each other.

In the case of 250 mJ/cm^2, the increase of absolute etch depth and of the difference between both profiles obtained by two different configurations ceased almost at the end of the excimer laser pulse ($\Delta t \sim +80$ ns). The exothermic thermal degradation is expected to sustain the temperature and continue the etching of the film even after the end of the excimer laser irradiation. However, the etching process was not clearly observed after the end of the excimer laser pulse, suggesting that the polymer is instantaneously decomposed mainly via the photochemical pathway as reported before.[21,22] On the other hand, for a fluence of 60 mJ/cm^2, the etching process continued until +140 ns as shown in Figure 4. The time-dependent etching behavior differed from that for the fluence of 250 mJ/cm^2, and the etching ceased about 60 ns after the end of the excimer laser irradiation ($\Delta t \sim +140$ ns). The prolonged etching after finishing excimer laser irradiation implies that not only the photochemical pathway of the decomposition of triazenopolymer but also some delayed decomposition are involved for the lower fluence of 60 mJ/cm^2. When laser fluence is high enough, photodecomposition occurs densely leading to sudden ablation, so that thermal degradation cannot be observed. On the other hand, at 60 mJ/cm^2 the thermal process was successfully measured as photodecomposition is suppressed. Here we remember that the decomposition of the triazenopolymer is an exothermic reaction.[21] Photodecomposition of the polymer results in the temperature elevation, causing thermal degradation. It is critical to determine the relative contribution of photochemical and photothermal processes upon laser ablation, and the direct measurement of the fluence-dependent etching behavior makes it possible to discuss and decide upon it.

Refraction Index Change in the Surface Layer. As shown in Figure 5, the increase of the transmission was stopped once and the transmission began to be attenuated from $\Delta t \sim +10$ ns. The transmission was decreased and reflectance was recovered in the range of +10 to +100 ns, while the permanent etching of 600 nm was already attained at the end of the excitation pulse by the nanosecond interferometry for a fluence of 250 mJ/cm^2. Thus, it is considered that the effective refractive index change at the surface layer, which first decreased and recovered to some extent, suggests that ejected gaseous products are responsible for the optical behavior.

In Figure 5b, time evolution of transmission and reflectance is shown for a fluence of 50 mJ/cm^2. The transmission increase was also observed, although the dynamics was different from that of 260 mJ/cm^2. Transmission and reflectance began to change from $\Delta t \sim -10$ ns, which is slower than that of 260 mJ/cm^2. The transmission decreases and small recovery of attenuated reflectance gradually continues up to 200 ns, while the permanent etching was completed around 140 ns. This again suggests the contribution of gaseous products to effective refractive index change, although the nature is still beyond our knowledge.

Laser Ablation Mechanism of Triazenopolymer Film. Laser ablation dynamics of a photosensitive triazenopolymer film at 250 and 60 mJ/cm^2 was revealed by using the nanosecond interferometric technique with a newly developed optical setup, as well as time-resolved transmission and reflectance measurements. As the new setup was free from the disturbance of ejected gas or debris, we could evaluate the photoetching process correctly. On the basis of the revealed etching dynamics of the film, the ablation mechanism of the triazenopolymer upon XeF excimer laser irradiation was discussed in detail, where photochemical and photothermal decomposition were competitive and the latter contribution was confirmed clearly only at low fluence.

It is quite interesting that the etching of the film did not start from the beginning of the excimer laser pulse for both fluences, although the photodecomposition of the triazenopolymer is believed to be induced on the ground of the darkening that started almost from the onset of the excimer laser pulse. The starting time of the etching for the fluence of 250 mJ/cm^2 was about Δt +10 ns, while about Δt +30 ns for the fluence of 60 mJ/cm^2. If the decomposed products were ejected instantaneously, time-dependent etched depth would obey the integration curve of the applied excimer laser pulse (thin dashed lines in the Figures 3 and 4). The delay of the etch profile to the excimer laser means that etching of the film cannot be initiated unless triazenopolymer is decomposed to some extent. It has been shown that only gaseous products with no debris were ejected upon ablation,[17,20] which suggests that the polymer is decomposed successively in the solid film until the initiation of the detectable etching process. Namely, explosive ejection of ablated polymer would be initiated and etching of the polymer

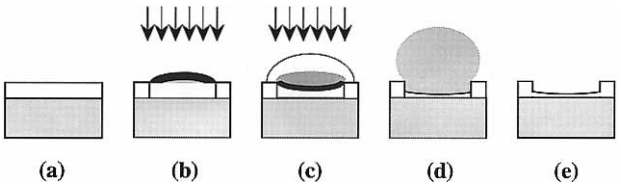

Figure 6. Schematic diagram of laser-induced decomposition and ablation dynamics of the photosensitive triazenopolymer film: (a) before excimer laser irradiation, (b) slight expansion of the film and darkening of the irradiated surface at the beginning of the excimer laser pulse, (c) initiation of etching of the film and ejection of gaseous fragments decomposed from the polymer, (d) completion of the etching and expansion of ejected plume, and (e) after the ablation.

film would be brought about after the triazenopolymer decomposed to a certain amount of gaseous low molecular weight products.

The present results on laser-induced decomposition and ablation dynamics of the triazenopolymer film are schematically summarized in Figure 6. At the beginning of excimer laser pulse, a slight expansion of the film and a darkening of the irradiated film surface were observed prior to etching of the film for the fluences of both 250 and 60 mJ/cm^2 (Figure 6b). Then etching of the film was initiated; however, the starting time depended on the applied fluence. The termination of the etching process was also affected by the applied laser fluence. It seemed to stop at +80 ns, which is almost the end of the excitation laser pulse, for the fluence of 250 mJ/cm^2, while it continued until +140 ns for a fluence of 60 mJ/cm^2 (Figure 6d). The fluence-dependent photoetching dynamics indicates that not only photochemical reactions but also photoinitiated thermal reactions are involved in the ablation process of the triazenopolymer film.

Acknowledgment. The present work was partly defrayed by a Grand-in-Aid from the Japanese Ministry of Education, Science, Sports, and Culture (07554063, 08454223). T.L. expresses his gratitude to the A. v. Humboldt Foundation and the Science Technology Agency (STA) of Japan for a research fellowship.

References and Notes

(1) Srinivasan, R.; Braren, B. *Chem. Rev.* **1989**, *89*, 1303.
(2) Miller, J. C., Haglund, R. F., Jr., Eds. *Laser Ablation—Mechanism and Applications*; Springer: New York, 1991.
(3) Miller, J. C., Eds. *Laser Ablation—Principles and Applications*; Springer: Berlin, 1994; Chapter 5.
(4) Chen, S.; Lee, I.-Y.; Talbert, S. W. A.; Wen, X.; Dlott, D. D. *J. Phys. Chem.* **1992**, *96*, 7178.
(5) Fukumura, H.; Takahashi, E.; Masuhara, H. *J. Phys. Chem.* **1995**, *99*, 750.
(6) Fukumura, H.; Mibuka, N.; Eura, S.; Masuhara, H.; Nishi, N. *J. Phys. Chem.* **1993**, *97*, 13761.
(7) Tsuboi, Y.; Hatanaka, K.; Fukumura, H.; Masuhara, H. *J. Phys. Chem.* **1994**, *98*, 11237.
(8) Fujiwara, H.; Fukumura, H.; Masuhara, H. *J. Phys. Chem.* **1995**, *99*, 11844.
(9) Tsuboi, Y.; Fukumura, H.; Masuhara, H. *J. Phys. Chem.* **1995**, *99*, 10305.
(10) Hare, D. E.; Dlott, D. D. *Appl. Phys. Lett.* **1994**, *64*, 715.
(11) Lippert, T.; Koskelo, A.; Stoutland, P. O. *J. Am. Chem. Soc.* **1996**, *118*, 1151.
(12) Fujiwara, H.; Hayashi, T.; Fukumura, H.; Masuhara, H. *Appl. Phys. Lett.* **1994**, *64*, 2451.
(13) Srinivasan, R.; Braren, B.; Casey, K. G.; Yen, M. *Appl. Phys. Lett.* **1989**, *55*, 2790.
(14) Srinivasan, R.; Braren, B.; Casey, K. G.; Yen, M. *J. Appl. Phys.* **1990**, *67*, 1604.
(15) Gilgenbach, R. M.; Ventzek, P. L. G. *Appl. Phys. Lett.* **1991**, *58*, 1597.
(16) Srinivasan, R. *J. Appl. Phys.* **1993**, *73*, 2743.
(17) Bennett, L. S.; Lippert, T.; Furutani, H.; Fukumura, H.; Masuhara, H. *Appl. Phys.* **1996**, *B63*, 327.
(18) Furutani, H.; Fukumura, H.; Masuhara, H. *Appl. Phys. Lett.* **1994**, *65*, 3413.
(19) Furutani, H.; Fukumura, H.; Masuhara, H. *J. Phys. Chem.* **1996**, *100*, 6871.
(20) Furutani, H. Ph.D. Thesis, Osaka University, 1997.
(21) Lippert, T.; Stebani, J.; Ihlemann, J.; Nuyken, O.; Wokaun, A. *J. Phys. Chem.* **1993**, *97*, 12296.
(22) Lippert, T.; Stebani, J.; Ihlemann, J.; Nuyken, O.; Wokaun, A. *Angew. Makromol. Chem.* **1993**, *206*, 97.